

THE SIZE OF "SECONDARY" DROPLETS WHEN A LIQUID IS ATOMIZED BY A ROTATING DISC

V. F. Dunsikii and N. V. Nikitin

UDC 66.069.8

We investigate the "second" regime of liquid atomization by means of a rotating disc, with this regime characterized by the formation of droplets of uniform size. It is this phenomenon that is of interest for engineering processes. Formulas suitable for practical calculations are proposed.

In the atomization of liquids – one of the most common engineering processes – the effort is generally toward the attainment of droplets of a specific optimum size; however, most atomizers form polydisperse systems of droplets with a wide range of sizes, which does not lend itself to control. In this connection, there is some interest in rotating atomizers which, under certain conditions, provide for uniform size in the droplets that are formed.

We know [1-4] that the atomization of a liquid by means of a smooth rotating disc or cone involves three different atomization regimes. At very low liquid flow rates approximately identical droplets are formed at the edge of the disc and these are known as "primary droplets" (the first regime).^{*} As the liquid flow rate is increased, the first regime is replaced by the second, in which we no longer find individual droplets at the edge of the disc, but continuous liquid filaments. At some distance from the edge of the disc these filaments break down into "secondary" droplets, less uniform in size than the primary droplets. Finally, with a further increase in the liquid flow rate the second regime of atomization is replaced by a third, in which it is no longer the individual liquid filaments that are thrown out from the edges of the disc, but a solid film; when subjected to perturbations this film can be broken down into droplets of different sizes.

The first atomization regime is frequently used in laboratory experiments; because of the low liquid flow rate at which this regime is achieved, for all intents and purposes, it cannot be used in engineering processes.

In the third atomization regime, the polydispersion ratio is approximately the same as for the other atomizers (hydraulic, pneumatic), so that the use of disc atomizers operating in the regime introduces nothing that is fundamentally new to atomization technique.

According to [1], the boundary separating the "monodisperse" region of atomization (the first and second regimes, relatively uniform droplet size) from the "polydisperse" region (the third regime) is determined by the empirical formula

$$k = \frac{\rho Q^2 \omega^{1.2} \nu^{0.33}}{\sigma^{1.77} R^{1.37}} = 4.5.$$

When $k < 4.5$ we achieve either the first or second regimes; with $k > 4.5$ we achieve the third regime.

In connection with engineering processes, the greatest interest is shown in the second atomization regime which is characterized by the formation and breakdown of the liquid filaments, since the "secondary"

^{*}Smaller "droplet-satellites" are formed simultaneously, and their relative quantity increases as the liquid flow rate increases.

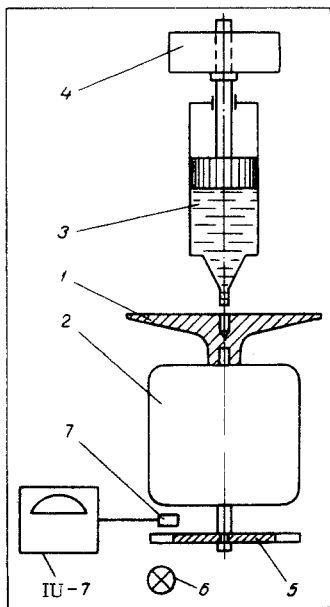


Fig. 1. Diagram of the experimental installation.

droplets formed in this regime are still quite uniform in size, and at the same time, this regime is achieved at increased liquid flow rates that are acceptable from the practical standpoint. This regime has not yet been adequately studied. Let us now examine it in greater detail.

The liquid is fed to the center of a rotating disc in a continuous jet which spreads out over the disc surface, forming a thin film whose thickness is measured in microns. As a result of the interaction between the centrifugal forces and the forces of surface tension, the liquid accumulates at the periphery of the disc in the form of a ring. The cross section of this ring may be assumed to be approximately circular, with the radius

$$a = \frac{1}{\omega} \left(\frac{\sigma}{2R\rho} \right)^{1/2}. \quad (1)$$

Formula (1) is in satisfactory agreement with the experimental data of [2].

The liquid ring at the edge of the disc, since it is unstable, is deformed by random perturbations, and for the determination of the "wavelength" (the most probable distance between the deforming sections of the ring) we can use the formulas applicable to the theory of liquid-jet decay ([5], p. 626); for a low-viscosity liquid ($\sqrt{a\sigma/\rho\nu^2} \gg 1$)

$$\lambda = 9a, \quad (2)$$

for a high-viscosity liquid ($\sqrt{a\sigma/\rho\nu^2} \ll 1$)

$$\lambda = 13 \sqrt[4]{\frac{\nu^2 \rho a^3}{\sigma}}. \quad (3)$$

In the general case, according to the approximate Weber formula [6],

$$\lambda = 9a \left(1 + \sqrt{\frac{4.5\nu^2\rho}{a\sigma}} \right)^{1/2}. \quad (4)$$

According to [2], if we assume that the filaments flow from the liquid ring at the edge of the disc precisely at the points of deformation, the number of filaments is given by

$$Z = \frac{2\pi R}{\lambda}. \quad (5)$$

According to results from spark photography [2], the liquid filaments are nearly involute in shape, i. e., the motion of an element of the filament is approximately described by the formula

$$S = 0.5R\omega^2 t^2. \quad (6)$$

Let us examine the process of a liquid filament disintegrating into droplets.

At some arbitrary cross section of the filament, because of its continuity, with consideration of (6),

$$\frac{Q}{Z} = \pi r^2 v = \pi r^2 \frac{dS}{dt} = \pi r^2 R \omega^2 t,$$

from which the radius r of the filament cross section, corresponding to its length S , is given by

$$r = \sqrt{\frac{Q}{\pi Z R t \omega^2}}. \quad (7)$$

In the case of a low-viscosity liquid ($\sqrt{r\sigma/\rho\nu^2} \gg 1$), according to (1), (2), and (5)

$$Z = R\omega \left(\frac{\rho R}{\sigma} \right)^{1/2}. \quad (8)$$

The time for the disintegration of the filament into droplets (theoretically the time for the increase in the amplitude of the axisymmetric perturbation by a factor of e , [5], p. 626),

$$t_p = 8.5 \sqrt{\frac{\rho r^3}{\sigma}}. \quad (9)$$

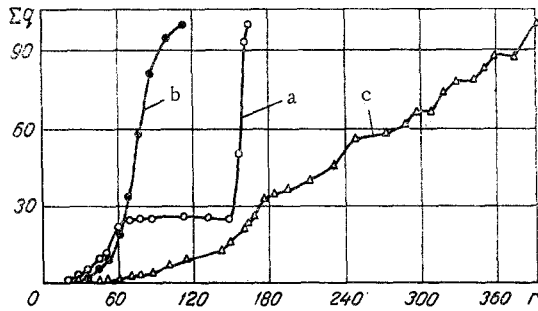


Fig. 2. Integral curves for droplet size distribution (motor oil is used as the liquid, $\omega = 314 \text{ sec}^{-1}$, $R = 3.5 \text{ cm}$): a) first atomization regime, $Q = 0.1 \text{ cm}^3/\text{sec}$; b) second regime, $Q = 0.5 \text{ cm}^3/\text{sec}$; c) third regime, $Q = 3.3 \text{ cm}^3/\text{sec}$.

Having substituted the values of Z and t from (8) and (9) into (7), for the filament radius at the point of decay we derive the expression

$$r_d = 0.39 \left(\frac{Q\sigma}{\rho\omega^3 R^{5/3}} \right)^{2/7}. \quad (10)$$

The unknown radius x for the "secondary" droplets formed as a result of the decay of a filament of radius r_d into cylinders of height $\lambda = 9r_d$ is

$$x_1 = 0.74 \left(\frac{Q\sigma}{\rho\omega^3 R^{5/2}} \right)^{2/7}. \quad (11)$$

The length of the nondecaying portion of the filament, according to (6) in conjunction with (9) and (10), is given by

$$S_d = 2.3 \left(\frac{Q^6 \rho}{R^3 \omega^4 \sigma} \right)^{1/7}. \quad (12)$$

In the case of an extremely viscous liquid ($\sqrt{r_d \sigma / \rho \nu^2} \ll 1$), according to [5], p. 626, if we assume that

$$t_d = \frac{5\nu\rho r}{\sigma}, \quad (13)$$

from similar calculations we obtain

$$x_2 = 1.06 \frac{\sigma^{0.27} Q^{0.306} \nu^{0.014}}{\rho^{0.27} R^{0.725} \omega^{0.84}}, \quad (14)$$

$$S_{d2} = 5.4 \left(\frac{\omega^2}{R^7} \right)^{1/12} \left(\frac{\rho}{\sigma} \right)^{5/4} \nu^{5/3}. \quad (15)$$

To test the derived formulas giving the radius of the "secondary" droplets, we performed tests on the installation shown schematically in Fig. 1. A continuous liquid jet from a spray nozzle 3 whose plunger is acted on by weight 4 is directed at the central cylindrical depression of a smooth horizontal disc 1 set into rotation by means of electric motor 2. The disc is made of duralumin, with a radius $R = 3.5 \text{ cm}$; its working surface has been polished to eliminate the grooves visible to the naked eye. To measure the rotational velocity of the disc, a ring 5 is mounted at the lower end of the shaft of electric motor 2 and this ring is provided with slits to break up a light beam directed from an incandescent bulb 6 to the photoresistance 7. The frequency of the pulses generated by the photoresistance (i. e., the rotational velocity of the disc) was measured by means of a frequency meter and regulated with a rheostat. At 9 cm below the plane of the disc a Textolite sheet is set up with a radial rectangular slot to hold slides to collect the droplets formed at various distances from the axis of the disc. To ensure a constant dispersion coefficient for the deposited droplets, the slides were first covered with a thin silicone layer. During the operation of the atomizer, the slides were exposed to a slit shutter to prevent the deposition of an excessive number of droplets. The slides were then examined in a microscope and the deposited droplets were counted and measured for a specific area of the slide.

The tests were performed with two liquids: transformer oil ($\rho_{20} = 0.892 \text{ g/cm}^3$, $\nu_{20} = 0.218 \text{ cm}^2/\text{sec}$, $\sigma_{20} = 33.2 \text{ g/sec}^2$) and with motor oil ($\rho_{20} = 0.897 \text{ g/cm}^3$, $\nu_{20} = 26.4 \text{ cm}^2/\text{sec}$, $\sigma_{20} = 29 \text{ g/sec}^2$). The test results were used to determine the droplet size distribution; consideration was given here to the distance separating each slide from the axis of the disc rotation. By observing the ring of stained liquid on a horizontal sheet of paper, we proved the axisymmetrical nature of the process.

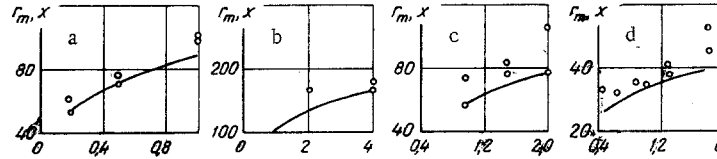


Fig. 3. Comparison of the calculated values for the radius x of the "secondary" droplets (curves) and the measured values of the median droplet mass radius r_m (the points): a) motor oil, $\omega = 314 \text{ sec}^{-1}$; b) transformer oil, $\omega = 157 \text{ sec}^{-1}$; c) transformer oil, $\omega = 314 \text{ sec}^{-1}$; d) transformer oil, $\omega = 628 \text{ sec}^{-1}$.

TABLE 1. Conditions for Experimentation and Derivation of Values for the Median Droplet Mass Radius

Liquid	Motor oil			Transformer oil										
	314			157		314			628					
ω, sec^{-1}														
$Q, \text{cm}^3/\text{sec}$	0,2	0,5	1,0	2,0	4,0	1,0	1,5	2,0	0,5	0,7	0,9	1,0	1,3	1,8
$r_m, \mu\text{m}$	60	75	97	165	165	55	76	103	—	—	—	—	38	45
	52	72	100	165	172	73	82	125	33	33	35	35	41	53

During the tests we varied the velocity of disc rotation (157, 314, and 628 sec^{-1}) as well as the liquid flow rate (from 0.05 to $4 \text{ cm}^3/\text{sec}$). Figure 2 shows typical integral curves for the distribution of droplet sizes, determined with a specific liquid (motor oil) at a constant rotational velocity (3000 rpm) and for various liquid flow rates. At a low flow rate, $Q = 0.1 \text{ cm}^3/\text{sec}$ (Fig. 2a), we find the first atomization regime: $\sim 25\%$ of the liquid is contained in fine "satellite" droplets with a radius ranging from 15 to 75μ . with the remaining 75% included among the "primary" droplets, i. e., droplets that are approximately identical, exhibiting a radius from 150 to 165μ .

With an elevated flow rate, $Q = 0.2-1 \text{ cm}^3/\text{sec}$, we noted the second atomization regime (Fig. 2b, $Q = 0.5 \text{ cm}^3/\text{sec}$): 80% of the liquid is contained in "secondary" droplets, relatively uniform in size (with the radius ranging from 55 through $95 \mu\text{m}$). Despite the elevated liquid flow rate, and all other conditions being equal, the "secondary" droplets are smaller than the primary droplets, which corresponds to the above concepts with regard to the mechanism of the process.

With an even greater flow rate, $Q > 2 \text{ cm}^3/\text{sec}$, we noted a third atomization regime — the formation of a polydisperse droplet system that is characteristic for conventional atomization devices (Fig. 2c, $Q = 3.3 \text{ cm}^3/\text{sec}$, with 80% of the liquid found in droplets with a radius ranging from 125 through $375 \mu\text{m}$).

For purposes of comparison with the theoretical formulas, we took the values of the median droplet mass radius r_m , derived in the experiments performed in the second atomization regime. The conditions under which these tests were conducted and under which we derived the values of r_m are listed in the table.

The results of the tests and the calculations (in accordance with (14) for motor oil and in accordance with (11) for transformer oil) are shown in Fig. 3. Satisfactory agreement was achieved.

We see from (11) and (14) that the liquid viscosity has little effect on the size of the "secondary" droplet; this was experimentally confirmed (Fig. 3). However, formula (15) shows that the viscosity has a pronounced effect on the length of the filament section that does not disintegrate; this was confirmed in tests with a highly viscous liquid, and here the thin liquid filaments that did not disintegrate were tens of centimeters in length and were visible to the naked eye. According to (15), for the atomization of a highly viscous liquid we should use discs with large radii; for the formation of long filaments (for example, to produce fibrous products) we should, conversely, use small-radius discs.

On the whole, the derived results demonstrate the validity of the assumed mechanism for the process, as well as the suitability of the proposed formulas for practical calculations.

NOTATION

R and ω are, respectively, the radius and the angular velocity of disc rotation;
 ρ , ν , σ , and Q are, respectively, the density, the kinematic viscosity, the surface tension, and the flow rate of the liquid;

a is the cross-sectional radius of the liquid ring at the disc periphery;
 λ is the wavelength;
 Z is the number of filaments;
 S is the filament length;
 t is the time;
 v is the average velocity of motion for a filament element;
 r is the filament radius;
 x is the radius for the "secondary" droplet.

LITERATURE CITED

1. J. Hinze and H. Milborn, *J. Appl. Mech.*, 17, 145 (1950).
2. H. Hege, *Chemie-Ing. Techn.*, 36, 52 (1964).
3. W. Walton and W. Prewett, *Proc. Phys. Soc. (London)*, 62B, 341 (1949).
4. V. F. Duskii and N. V. Nikitin, *Inzhen.-Fiz. Zh.*, 9, 54 (1965).
5. V. G. Levich, *Physicochemical Hydrodynamics* [in Russian], Fizmatgiz, Moscow (1959).
6. K. Weber, *Z. angew. Math. Mechanik.*, 11, 136 (1931).